Journal of Applied and Computational Mechanics, Vol. 1, No. 3, (2015), 145-151
DOI: 10.22055/jacm.2015.10999

Journal of
Applied and Computational Mechanics

Computation of slip analysis to detect adhesion for the protec tion of rail vehicle derailment

Zulfiqar Ali Soomro

Department of Mechanical Engineering; Post-graduate Studies, Mehran University of Engineering. &Tech;
Jamshoro (Sindh)-76062 Pakistan. zulfiqarali_s@yahoo.com.

Received: December 06 2014; revised February 21 2015; accepted for publication February 11 2015.
Corresponding author: zulfiqarali_s@yahoo.com.

Abstract

Adhesion level for the proper running of rail wheelset on track has remained a significant problem for researchers in detecting slippage to avoid accidents. In this paper, the slippage of rail wheels has been observed applying forward and lateral motions to slip velocity and torsion motion. The longitudinal and lateral forces behavior is watched with respect to traction force to note correlation based on the angle of attack. The deriving torque relation with tractive torque is watched to check slippage. Coulomb's law is applied in terms of tangential forces to normal forces owing to creep co-efficient and friction to get the adhesion. Nadal's limiting ratio is applied to escape from wheel climb and derailment from track depending upon wheel profile and flange on straight path and curves.

Keywords: Traction, torsion, creep forces, angle of contact, creep co-efficient, friction

1 Introduction

The rolling contact phenomena, creepages on wheel/rail contact, and creep force models for longitudinal train dynamics are presented in this paper [1]. The authors have proposed a re-adhesion control scheme that blends two conventional methods: motor current control and slip speed control. If one method fails, the other will be activated. If both fail (usually when all wheels are simultaneously slipping), the estimated acceleration criterion control will be activated. This control scheme is based on the estimation of the reference speed of a bogie. The reference speed is estimated using speed sensors on two axles of a bogie and two axles on an adjacent bogie, and is then compared with an extra train speed indicator [2, 3]. If the reference speed is less than the wheel speed from the speed indicator, it is allowed to increase according to the estimated train acceleration. If the reference speed is greater than the wheel speed from the speed indicator, it is allowed to decrease according to the estimated train acceleration. The researchers have verified the proposed control method using a downscaled simulator. The results show the performance of the control method with a lot of oscillations. Also, regaining adhesion is time-consuming. Based on these results, this control method may not be efficient in high-speed trains as proposed. In addition, it is mainly based on the estimation of the train reference speed and train acceleration, using wheel speeds and a speed indicator. Watanabe and Yamashita [4] have presented an anti-slip re-adhesion control method using vector control without speed sensor. Also, the study includes only a sudden drop of 10% of adhesion force that is not sufficient to prove the efficiency of the control method. Mei, Yu, and Wilson have proposed a new approach for wheel slip control [5]. The study is based on the detection of torsional vibration of a wheelset when slipping.

The adhesion coefficient depends upon the slip velocity or slip also known as slip adhesion. The slip velocity has influence upon adhesion coefficient level of zero to higher value. The railway surfaces depend upon a train velocity and temperature of contact area. The maximum of the adhesion coefficient occurs on higher value of the adhesion coefficient and the slip velocity. The other parameter acting upon the value of the tangential force affects the alteration of the adhesion weight. These alterations occur when the locomotive, through a switch or crossing like pitches, bounces or moves [6].

Since Nadal's pioneering work a century ago, many studies have shown that Nadal's limit is extremely conservative for most practical cases (see Gilchrist and Brickle (1976) [7], Cheli et al.[2003]). Gilchrist and Brickle

(1976) [8] applied Kalker's theory of creep in a re-examination of Nadal's analysis, showing that Nadal's formula is suitable for the most pessimistic situations when the longitudinal creep on the flange is smaller and the angle of attack is larger. Most recent research on wheel derailment phenomena can be found in Barbosa (2004) [9], Wu et al. (2005) [10] and Braghin et al. (2006) [11]. This paper presents the behavior of velocity, creep forces for detection of slip by adhesion and Nadal's limiting ratio to avoid train derailment.

2. Dynamics of wheelset

When longitudinal creep is zero in a pure rolling case, no tangential force is transmitted on the area of contact. When a slip region appears in the trailing edge of the contact, the patch tangential forces are transmitted, while the remaining contact patch sticks in rolling–sliding contact patch. On increasing creep, the slip region increases on the decrease of stick region in size. The stick region vanishes, leading to gross slip on the higher creep. The relationship between creep and tangential force is shown in Fig-1 [12,13].

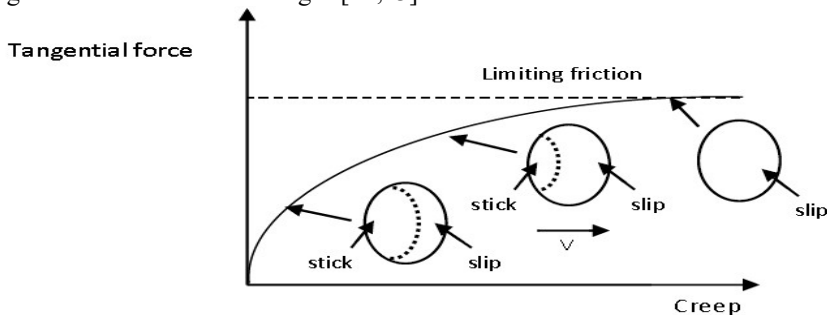

Fig. 1. Slip behavior on limiting friction of tangential force to creep

2.1 Slip velocity

The slip velocity, defined in Equation-1, is the most important factor influencing adhesion. The adhesion coefficient becomes higher if the slip velocity is controlled effectively [13]. This denotes that various reference slip velocities depend on the current rail condition. Much experimental work has been done to derive a general relationship for how slip velocity affects the adhesion coefficient, and thereby the adhesive force [13, 28]. The slip causes the difference between the longitudinal velocity and angular velocity of the wheelset. We use the following definition of slip:

$$S = (w.r - v)/v \tag{1}$$

where r is the radius of the wheel, ω the angular velocity of the wheel and v the longitudinal velocity of the vehicle. In the numerator of Equation (1), we define slip velocity as V_s, i.e.,

$$V_s = (w.r - v) \tag{2}$$

Sometimes a separate definition of the slip is used when the slip velocity is negative. This is often called slide, but we choose to refer to it as negative slip. In railway vehicles the traction procedure is slightly different. First, there are no rubber tires on the wheels, but metal both in the rail and in the wheels. As explained above, the slip is necessary to transmit the motor torque into vehicle movement. The explanation of railway vehicle slip is given by [14] which is due to the massive weight of the railway vehicle. Both the wheels and the rail expand and contract in different regions.

2.2 Adhesive Force

A general scientific definition of the adhesive force is attachment between two contacting surfaces. Also, it can be defined as the ability of the wheel to higher tractive force on the rail to maintain existence of contact free of exceeding the optimal slip [15]. The adhesive force is given by:

$$F_a = \mu_a.N = \mu_a.m_a.g \tag{3}$$

where F_a is the adhesive force, μa the adhesion coefficient, N the normal force, m_a the adhesive mass of the vehicle and g the gravitational constant.

2.3 Longitudinal Creepage

Let us consider a wheelset deflected laterally from a pure rolling position by a distance '*y'* (Figure -2) as the "Initial State" while on straight track, with the pure rolling position as the centerline of the track. On rolling forward with a velocity *v*, the deflected wheelset will tend to roll to "Preferred State". If the wheelset is constrained to remain in a similar attitude to the track, as it was in the "Initial State," creepage/slip takes place as the wheels roll [16]. In the case illustrated, the wheel of larger rolling diameter slips back with the smaller rolling diameter wheel slipping forward. Longitudinal creepage is defined as the ratio of the creep velocity to the forward velocity of wheelset. Slip forces, Fs are generated on the wheelset, which react against the constraining forces at the journals. Forces opposite to Fs are acting on the rail. The amount of creepage and the creep force generated are directly proportional to the displacement y and the cone angle γ.

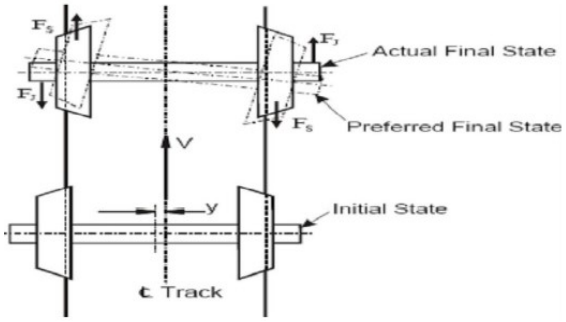

Fig. 2. Slip of wheelset on track on application of longitudinal force.

The effects of longitudinal creepage are very commonly observed in running track. Excessive longitudinal creepage, combined with high-contact stresses, is often seen in material flow of the rail producing head checks and subsequent shelling [17].

2.4 Lateral Creepage

Consider a wheelset placed at an angle of attack (angle of yaw), α, on the track (Figure -3). As the wheelset rolls forward, the preferred final state of the wheelset is shown by the dotted line. If the wheel is constrained by the vehicle suspension or a flange force to be oriented to the track in a similar position as the initial state, the wheelset must have slipped laterally. This is called lateral creepage/slip and the associated forces are lateral creep force [18].

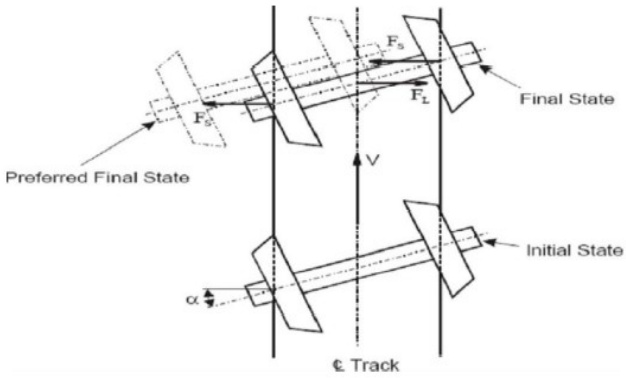

Fig. 3. Slippage of the wheelset on track for lateral force application.

In case the wheelset is not fully constrained in the lateral direction, the creepage reduces the lateral velocity V_t of a wheel due to its rotational velocity is given by:

$$V_t = -\omega.r_o.\sin(\alpha) \tag{3}$$

where r_o is rolling radius and α is wheelset angle of attack.

Figure -3 shows a plan view of a wheelset with an Angle of Attack, α relative to the track. This angle yields to the lateral creepage by a component of the wheelset's rotational velocity. If the wheelset has a lateral velocity, ẏ, with component of lateral velocity due to its rotation, the net lateral velocity of the wheelset at the contact zone, for small angle of attack (α = sin α), is given by:

$$V_y = \dot{y} - \omega.r_o..\alpha \tag{4}$$

Lateral creepage is the wheel-rail relative lateral velocity divided by the forward velocity:

$$\gamma_y = (\alpha - \dot{y}/v) \tag{5}$$

The term (α - ẏ/V), known as the 'effective angle of attack', is a function of the lateral velocity of the wheelset. Thus, the lateral velocity tends to reduce the effective angle of attack if the wheelset is moving towards flange contact with a positive angle of attack. The effective angle of attack force is proportional to and associated with lateral creepage. The constant of proportionality is dependent, inter alia, on axle load and contact geometry. Further, Spin slip or creepage acts upon lateral creep force. The direction of lateral creep force depends upon the resultant of the combination of both lateral and spin creepages. However, the effect of spin creep is small.

2.5 Wheel climb/ derailment

When one of the wheels rolls over the rail to the outside part of the track, this is called wheel flange climb

derailment. Various formulae exist for the analysis of this derailment process, in which analysis of railway vehicle dynamics give the ratio between the lateral and vertical forces for a particular wheel/rail combination. This ratio is usually called the "derailment ratio", displayed here as *Y/Q* (also known as *L/V* ratio), where *Y* (*L*) and *Q* (*V*) are the lateral and vertical forces in the flange contact, respectively. The derailment ratio *Y/Q* is used as a measure of the running safety of a railway vehicle. Several theories have been developed to establish the *Y/Q* ratio. One of the most widely used is the Nadal [1908] derailment criterion which describes the conditions necessary to sustain equilibrium of the forces in flange contact. Description of the Nadal theory can be found in Dukkipati (2000) [19]. This principle is expressed in Nadal's formula:

$$Y / Q = (\tan \alpha 1 - \mu) / (1 + \mu \tan \alpha 1) \tag{6}$$

Where α1 is the angle between the wheel flange and horizontal line and μ is the friction coefficient. The wheel flange angle is defined as the maximum angle of the wheel flange relative to the horizontal axis, as illustrated in Figure-4, where α1 is shown as α .

The wheelset will have a large lateral velocity under the influence of the derailing lateral forces at small angle of attack, up to 5 m-rad, then Effective Angle of Attack, (ά – ŷ/V), would be -ve resulting in the generation of a lateral creep force to oppose the derailment on the non-flanging wheel depending upon the magnitude of this lateral force upon the Effective Angle of Attack. Hence, the criteria as per Nadal equation may be conservative at small Angles of Attack.

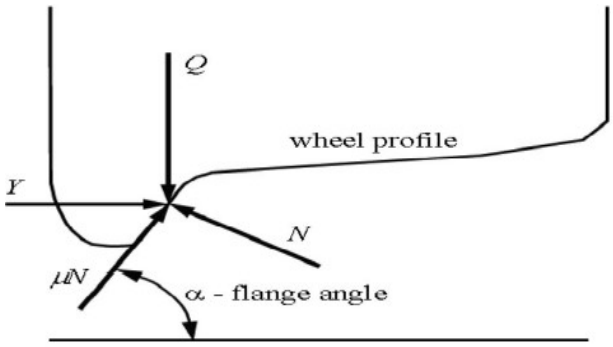

Fig. 4. Lateral and Normal force action upon on wheel profile.

3. Simulation Results

In the first part of Figure-5 below, the linear and angular velocities of the rail wheel se contact have been displayed. Here it can be observed that linear velocity of the right wheel and angular velocity of the left wheel nearly overlap in straight path with little deflection. However, angular velocity of the right wheel aparts parallel with slight deflection over linear velocity of the left wheel.

In the second quadrant of Figure-5, the tracking system of the vehicle has been correlated with the angular velocities of left and right wheels. Here curves for angular velocities of wheelset travel parallel with each other having small deflection to the tracking velocity between them in the straight line. However, the forward motion of the wheels deflects smaller to the straight path of the traction.

In the third portion of Figure-5, the forward velocity and traction (axle) velocity of the railway vehicle for wheelset dynamics have been simulated. Here longitudinal (forward) velocity of railway train and that of axle speed have been displayed in black and blue, respectively. The forward velocity of rail wheel starts from 0 to rise upward with slight inclination to finish its travel at nearly 180 m/s lower than 200 m/s in 1.4 seconds as shown in the graph. However, the torsional (axle) speed remains constant and does not show any variation in it to travel in the straight path at minor speed (say about 5-10 rad/sec in the range of 200 shown on vertical scale) above 0 rad/s for solid axle railway wheelset. To keep the balance between left and right rail wheel speed combination, there should not be any major difference in variation of axle speed with reference to them except higher speeds adapted by TALGO trains of Japan with independent rotating wheelset (IRW) axle system.

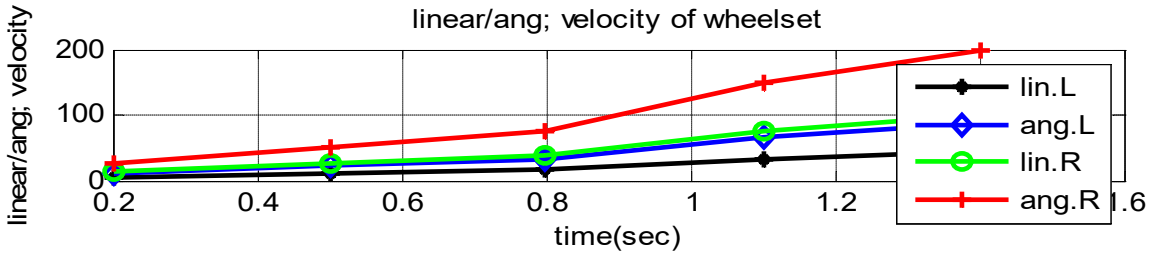

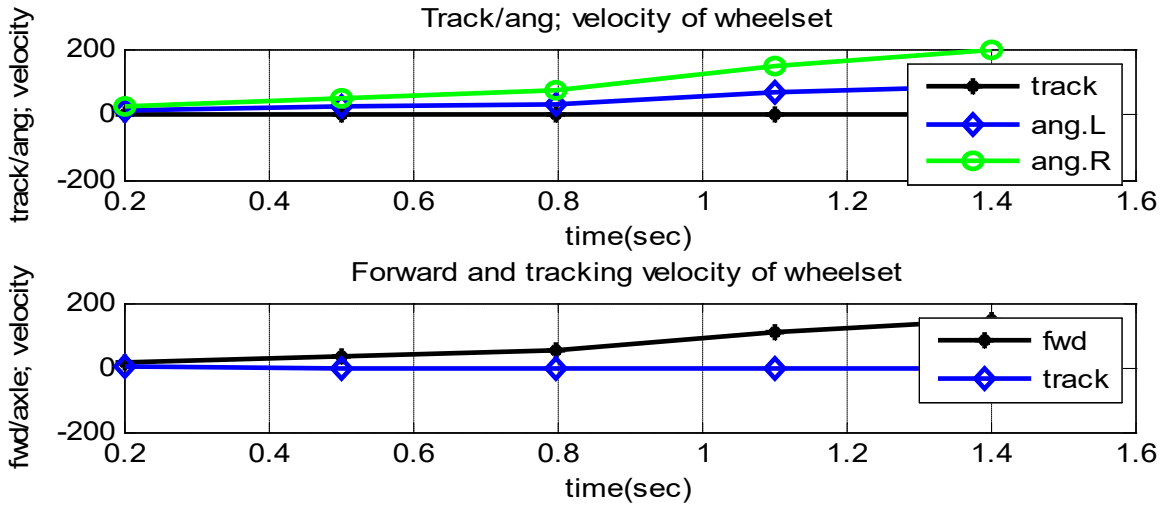

Fig. 5. Linear and angular velocity analysis of wheels on traction.

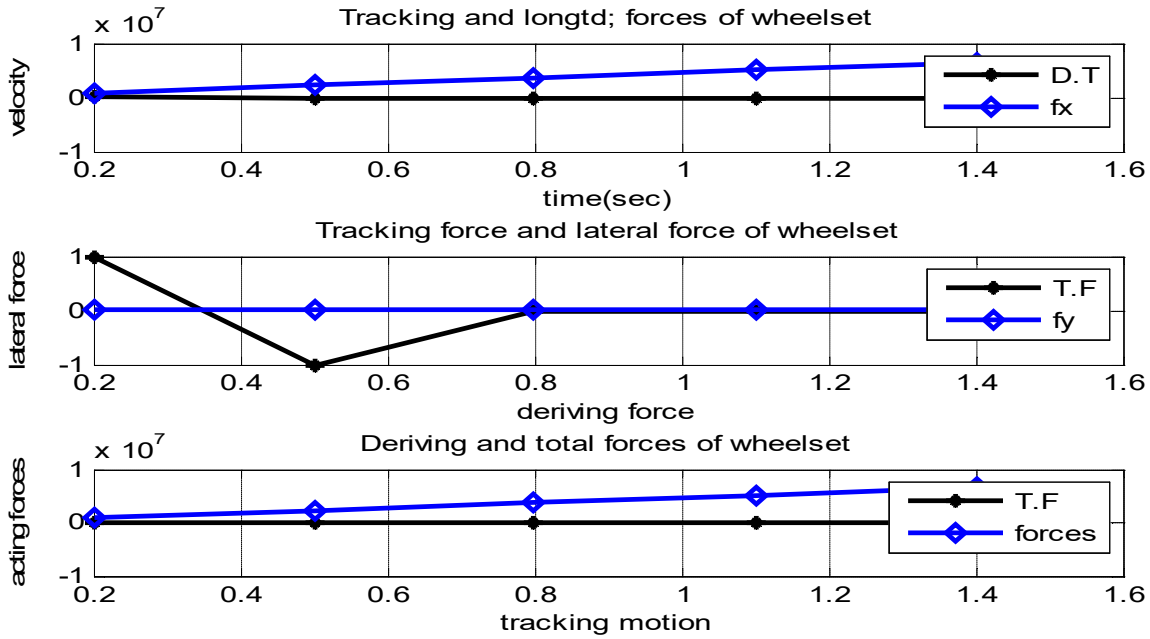

Fig. 6. Analysis of the applied forces to the tractive force on wheelset.

Figure-6, the longitudinal forces start form 0 parallel over the line of the traction force in straight line in its first portion. In the second part, the total forces curve starts from 1 to -1 n to end in a zigzag manner at 0 over the straight path of the lateral force in the same direction. The third quadrant represents the behavior of the acting total forces parallel to the tracking forces in the straight line starting from 0 to end on below 1e+7 N in 1.4 seconds.

The first portion of Figure-7 represents torsional torque of the axle and turning moments of the left and right wheels of the rail vehicle. Here the turning moments of the right wheel starts inversely nearly below 0 to 1e+10 N-m to end 0 in the straight line in 1.4 seconds. While left wheel moment starts above 0 to $-1*10^{10}$ then to zero to end in 1.4 sec to the tracking torque which starts from 0 in 0.8 sec when these two torques are joined with each other. Whereas in the second part, the deriving torque starts 0 in 0.2 second up to 1.4 sec on the same attitude of these two torques. The third part of this figure is of ample importance as the tangential forces are compared to the normal forces associated with co-efficient of the friction (μ) which supports the analysis of the adhesion level. Here the curve starts from minor above 0 to nearly lower 4000 N in normal forces on y-axis to nearly above 200 N to end nearly 1800 n of applied tangential forces in x-axis. This shows that adhesion increases linearly with the increase of these two tangential and normal forces.

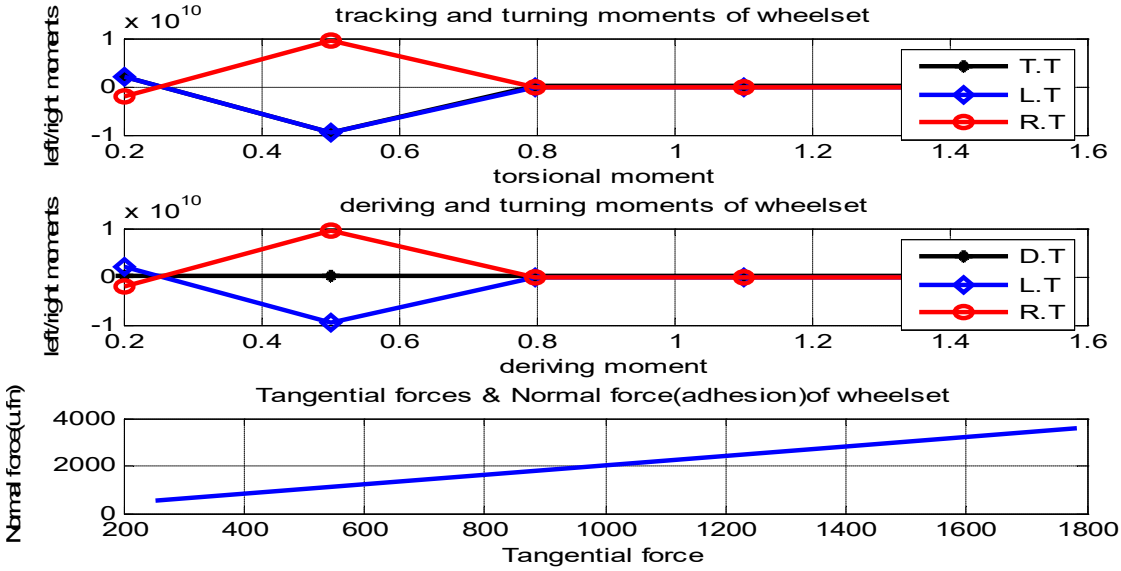

Fig. 7. Turning moments and Adhesion level for running wheelset

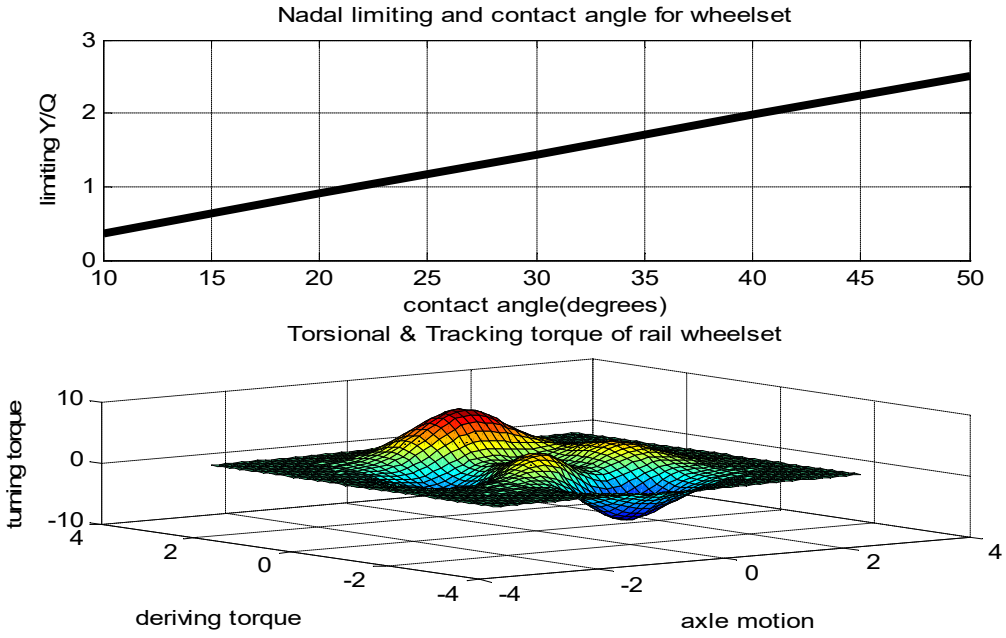

Fig. 8. Nadal's limiting ratio and torque analysis in 3-D environment.

The Nadal's limiting ratio is represented by lateral motion to vertical velocity (Y/Q) to various values for the angle of contact in degrees in the 1st part of figure-8. The Nadal's ratio varies linearly above 0.25 limiting ratio at vertical plane on 10 degrees for angle of contact at horizontal plane to end below 3 at approximately 2.5 of velocity ratio on 50 degrees at angle of contact in horizontal plane. This resembles the graph drawn by adhesion level detection in the 3rd part of Figure-7.

Whereas 3D diagram shown in the second part of Figure-8 represents the torsional motion in X-plane within -4 to 4 rad, deriving torque in Y-plane with the same scale and turning effect in Z-plane is within the range of -10 to 10 N-m. This second crucial part of Figure-8 is of great importance in representing the three important dynamic factors displayed. In addition, it resembles 'Zero-Pole diagram' for transfer function to check the stability of the model. The above humps show 'poles' and below humps denote 'zeros' as roots of denominator and numerator, respectively, in transfer function to control and fit input and outputs of black box models. The poles and zeros are usually displayed by s-plane. This type of graph represents transfer function usually called 'transfer curve', in which it has one pole and one zero. If pole is at the left side of the S-plane as in our graph, this means the model system is stable. This type of graph is preferable for most LTI (Linear Time Invariant) systems.

4. Conclusion

In this paper, the various possible occurring motions, i.e., axle, longitudinal, lateral and slip velocity have been discussed. Thus, slippage ratio of the rail wheelset has been enumerated by various techniques to detect the level of the adhesion to prevent hazardous accidents and wear. The tailor of wheelset slippage of rail wheelset from initial condition to final stage on rail track up to preferred position has been shown. The creepage forces for longitudinal and lateral with their velocities in terms of mathematical formulas are described. The adhesion level has been described and computed to detect slippage. Further, the Nadal's limiting ratio has been explained and applied by comparing the lateral and vertical velocities to avoid wheel derailment. Thus, various concerned parameters were applied to find out their relationship and behavior by computer simulation through results. The longitudinal and lateral velocities with respect to slip velocity and axle velocity are correlated. The behavior of longitudinal and lateral forces to track force is also graphed. Therefore, concerned moments of wheelset to torsional and tracking torque are determined to watch slippage. Thus, linear adhesion level is calculated by tangential and normal forces which show that their ideal condition to avoid slippage. While Nadal' limitation being conservative describes the derailment on climbation of flange wheelset due to whell/rail profile, the wheel profile design due to nadal ratio provides stability for high speeds on straight path.

References

[1] Kung, C., Kim, H., Kim, M. & Goo, B., "Simulations on Creep Forces Acting on the Wheel of a Rolling Stock." International Conference on Control, Automation and Systems, Seoul, Korea. Oct. 14 – 17, 2008.

[2] Hwang, D., Kim, M., Park, D., Kim, Y. & Kim, D. "Re-adhesion Control for High- Speed Electric Railway with Parallel Motor Control System." Proceedings of 5th International Conference, ISIE, IEEE International Symposium, Vol. 2, pp. 1024 – 1029, 2001.

[3] Hwang, D., Kim, M., Park, D., Kim, Y. & Lee, J. "Hybrid Re-adhesion Control Method for Traction System of High-Speed Railway." Proceedings of 5th International Conference, ISIE, IEEE International Symposium, Vol. 2, pp. 739 – 742 Aug. 2001.

[4] Watanabe, T. & Yamashita, M. "Basic Study of Anti-slip Control without Speed Sensor for Multiple Drive of Electric Railway Vehicles." Proceedings of Power Conversion Conference, Osaka, IEEE, Vol. 3, pp. 1026 – 1032, 2002.

[5] Mei, T., Yu, J. & Wilson, D. "A Mechatronic Approach for Effective Wheel Slip Control in Railway Traction." Proceedings of the Institute of Mechanical Engineers, Journal of Rail and Rapid Transit, Vol. 223, Part. F, pp. 295 – 304, 2009.

[6] Barbosa R.S., A 3D Contact Force Safety Criterion for Flange Climb Derailment of a Railway Wheel, Vehicle System Dynamics, Vol. 42, No. 5, pp. 289–300, 2004.

[7] Braghin F., Bruni S. and Diana G. (2006), Experimental and numerical investigation on the derailment of a railway wheelset with solid axle, Vehicle System Dynamics, Vol. 44, No. 4, , pp. 305–325. (2006)

[8] Chelli F., Corradi R., Diana G., Facchinetti A., Wheel–rail contact phenomena and derailment conditions in light urban vehicles. Proceedings of the 6th International Conference on Contact Mechanics and Wear of Rail/Wheel Systems. Gothenburg, Sweden, pp. 461-468, 10-13, 2003.

[9] Gilchrist A.O., Brickle B.V., A re-examination of the proneness to derailment of a railway wheelset, J. Mech. Eng. Sci., Vol. 18, pp. 131–141, 1976.

[10] Sawley K. and Wu H., The formation of hollow-worn wheels and their effect on wheel/rail interaction, Wear, Vol. 258, pp. 1179-1186, 2005.

[11] Kondo, K., Anti-slip control technologies for the railway vehicle traction," Vehicle Power and Propulsion Conference (VPPC), IEEE, pp.1306, 1311, 9-12 Oct. 2012

[12] Arias-Cuevas O., Low adhesion in the wheel–rail contact, Doctoral thesis, TUD, Delft, 2010 [1] E. Andersson and M. Berg. J¨arnv¨agssystem och sp°arfordon. KTH H¨ogskoletryckeri, Stockholm, Sweden, August 1999. In Swedish, (2010.

[13] Ishikawa, Y., Kawamurra, A., Maximum adhesive force control in super high speed train. IEEE, Proceedings of the Power Conversion Conference, Nagaoka, 2, pp. 951–954, August 1997.

[14] Takaoka, Y., Kawamura, A., Disturbance observer based adhesion control for shinkansen. IEEE, Proceedings, 6th International Workshop on Advanced Motion Control, pp. 169–174, 2000.

[15] S. Senini, F. Flinders, and W. Oghanna. Dynamic simulation of wheel-rail interaction for locomotive traction studies. Proceedings of the 1993 IEEE/ASME Joint Railroad Conference, pp. 27–34, April 1993.

[16] Nadal M. J., Locomotives a Vapeur, Collection Encyclopédie cientifique, Bibliothèque de Mécanique Applique´ et Génie, Paris, 1908.

[17] Dukkipati R.V., Vehicle Dynamics, Boca Raton: CRC Press, ISBN 0-8493-0976-X (2000).

[18] International Heavy Haul Association: Guidelines to Best Practices for Heavy Haul Railway Operations: Wheel and Rail Interface Issues, First Edition May 2001

[19]. International Heavy Haul Association: Guidelines to Best Practices for Heavy Haul Railway Operations, 2009: Infrastructure, Construction and Maintenance Issues 13. John Tuna and Curtis Urban, TTCI, Pueblo, Colorado, USA; IHHA 2007 Specialist Technical Session, Kiruna, 2009.